Supplementary Materials

Supplementary Tables

Supplementary Table 1.
RSA results based on the BABRI dataset

Variable	Shared	MCI-Specific	Comparison
Demographic characteristics			
Age	$\tau = 0.006$, $t(9) = 16.91$, $p < 0.001$	$\tau = 0.002$, $t(9) = 4.17$, $p < 0.001$	$\tau = -0.004$, $t(9) = -4.76$, $p < 0.001$
Sex	$\tau = 0.118$, $t(9) = 33.42$, $p < 0.001$	$\tau = -0.002$, $t(9) = -2.65$, $p < 0.001$	$\tau = -0.120$, $t(9) = -36.17$, $p < 0.001$
MCI-specific cognitive domains			
Episodic Memory	$\tau = -0.004$, $t(9) = -11.40$, $p < 0.001$	$\tau = 0.022$, $t(9) = 112.05$, $p < 0.001$	$\tau = 0.026$, $t(9) = 60.95$, $p < 0.001$
Attention	$\tau = -0.006$, $t(9) = -8.82$, $p < 0.001$	$\tau = 0.037$, $t(9) = 13.72$, $p < 0.001$	$\tau = 0.043$, $t(9) = 14.14$, $p < 0.001$
Executive Function	$\tau = -0.001$, $t(9) = -6.26$, $p < 0.001$	$\tau = 0.003$, $t(9) = 29.87$, $p < 0.001$	$\tau = 0.004$, $t(9) = 17.06$, $p < 0.001$
Shared cognitive domain			
General Cognition	$\tau = 0.009$, $t(9) = 28.20$, $p < 0.001$	$\tau = 0.001$, $t(9) = 5.94$, $p < 0.001$	$\tau = -0.008$, $t(9) = -25.93$, $p < 0.001$
Language	$\tau = 0.029$, $t(9) = 27.68$, $p < 0.001$	$\tau = 0.008$, $t(9) = 3.65$, $p = 0.005$	$\tau = -0.020$, $t(9) = -10.22$, $p < 0.001$

Supplementary Table 2.
RSA results from the internal validation set of BABRI

Variable	Shared	MCI-Specific	Comparison
Demographic characteristics			
Age	$\tau = 0.106$, $t(9) = 35.62$, $p < 0.001$	$\tau = 0.028$, $t(9) = 64.93$, $p < 0.001$	$\tau = -0.078$, $t(9) = -24.88$, $p < 0.001$
Sex	$\tau = 0.149$, $t(9) = 11.62$, $p < 0.001$	$\tau = -0.003$, $t(9) = -11.84$, $p < 0.001$	$\tau = -0.152$, $t(9) = -11.79$, $p < 0.001$
MCI-specific cognitive domains			
Episodic Memory	$\tau = -0.004$, $t(9) = -11.40$, $p < 0.001$	$\tau = 0.022$, $t(9) = 112.05$, $p < 0.001$	$\tau = 0.026$, $t(9) = 60.95$, $p < 0.001$
Attention	$\tau = -0.006$, $t(9) = -8.82$, $p < 0.001$	$\tau = 0.037$, $t(9) = 13.72$, $p < 0.001$	$\tau = 0.043$, $t(9) = 14.14$, $p < 0.001$
Executive Function	$\tau = -0.012$, $t(9) = -46.28$, $p < 0.001$	$\tau = 0.027$, $t(9) = 53.03$, $p < 0.001$	$\tau = 0.039$, $t(9) = 68.55$, $p < 0.001$
Shared cognitive domain			
General Cognition	$\tau = 0.012$, $t(9) = 10.19$, $p < 0.001$	$\tau = -0.006$, $t(9) = -314.25$, $p < 0.001$	$\tau = -0.018$, $t(9) = -15.05$, $p < 0.001$
Language	$\tau = 0.029$, $t(9) = 27.68$, $p < 0.001$	$\tau = 0.008$, $t(9) = 3.65$, $p = 0.005$	$\tau = -0.020$, $t(9) = -10.22$, $p < 0.001$

Supplementary Table 3.
RSA results based on the ADNI1 dataset

Variable	Shared	MCI-Specific	Comparison
Demographic characteristics			
Age	$\tau = 0.004$, $t(9) = 12.92$, $p < 0.001$	$\tau = 0.004$, $t(9) = 33.59$, $p < 0.001$	$\tau = -0.000$, $t(9) = -1.12$, $p = 0.290$
Sex	$\tau = 0.020$, $t(9) = 6.91$, $p < 0.001$	$\tau = -0.007$, $t(9) = -8.70$, $p < 0.001$	$\tau = -0.027$, $t(9) = -10.34$, $p < 0.001$
MCI-specific cognitive domains			
Episodic Memory	$\tau = 0.002$, $t(9) = 0.85$, $p = 0.416$	$\tau = 0.020$, $t(9) = 11.91$, $p < 0.001$	$\tau = 0.018$, $t(9) = 8.98$, $p < 0.001$
Attention	$\tau = -0.005$, $t(9) = -27.72$, $p < 0.001$	$\tau = 0.065$, $t(9) = 33.78$, $p < 0.001$	$\tau = 0.070$, $t(9) = 34.63$, $p < 0.001$
Executive Function	$\tau = 0.003$, $t(9) = 2.52$, $p = 0.033$	$\tau = 0.014$, $t(9) = 18.27$, $p < 0.001$	$\tau = 0.010$, $t(9) = 5.77$, $p < 0.001$
Shared cognitive domain			
General Cognition	$\tau = 0.021$, $t(9) = 27.02$, $p < 0.001$	$\tau = 0.003$, $t(9) = 4.95$, $p < 0.001$	$\tau = -0.018$, $t(9) = -20.21$, $p < 0.001$
Language	$\tau = 0.029$, $t(9) = 6.56$, $p < 0.001$	$\tau = 0.024$, $t(9) = 23.04$, $p < 0.001$	$\tau = -0.004$, $t(9) = -1.11$, $p = 0.296$

Supplementary Table 4.
RSA results from the combined ADNI2 and ADNI3 datasets

Variable	Shared	MCI-Specific	Comparison
Demographic characteristics			
Age	$\tau = 0.006$, $t(9) = 22.45$, $p < 0.001$	$\tau = -0.002$, $t(9) = -6.22$, $p < 0.001$	$\tau = -0.008$, $t(9) = -16.43$, $p < 0.001$
Sex	$\tau = 0.016$, $t(9) = 18.94$, $p < 0.001$	$\tau = -0.003$, $t(9) = -12.31$, $p < 0.001$	$\tau = -0.019$, $t(9) = -19.94$, $p < 0.001$
MCI-specific cognitive domains			
Episodic Memory	$\tau = 0.000$, $t(9) = 0.98$, $p = 0.351$	$\tau = 0.028$, $t(9) = 7.01$, $p < 0.001$	$\tau = 0.028$, $t(9) = 6.59$, $p < 0.001$
Attention	$\tau = 0.003$, $t(9) = 4.42$, $p = 0.002$	$\tau = 0.019$, $t(9) = 34.59$, $p < 0.001$	$\tau = 0.016$, $t(9) = 16.60$, $p < 0.001$
Executive Function	$\tau = 0.003$, $t(9) = 9.28$, $p < 0.001$	$\tau = 0.010$, $t(9) = 22.80$, $p < 0.001$	$\tau = 0.008$, $t(9) = 17.11$, $p < 0.001$
Shared cognitive domain			
General Cognition	$\tau = 0.029$, $t(9) = 8.24$, $p < 0.001$	$\tau = 0.012$, $t(9) = 18.64$, $p < 0.001$	$\tau = -0.017$, $t(9) = -4.53$, $p = 0.001$
Language	$\tau = 0.034$, $t(9) = 25.43$, $p < 0.001$	$\tau = 0.029$, $t(9) = 12.95$, $p < 0.001$	$\tau = -0.005$, $t(9) = -2.39$, $p = 0.041$

Supplementary Table 5.
Architecture of the CVAE model

Layer	Output Shape	# Param	Connected to
Shared Encoder			
inputs	(None,64,64,64,1)	0	-
conv3d	(None,32,32,32,64)	1792	inputs
conv3d_1	(None,16,16,16,128)	221312	conv3d
flatten	(None,524288)	0	conv3d_1
dense	(None,128)	67108992	flatten
z_mean	(None,16)	2064	dense
z_log_var	(None,16)	2064	dense
z (Lambda)	(None,16)	0	z_mean, z_log_var
MCI-specific Encoder			
inputs	(None,64,64,64,1)	0	-
conv3d_2	(None,32,32,32,64)	1792	inputs
conv3d_3	(None,16,16,16,128)	221312	conv3d_2
flatten_1	(None,524288)	0	conv3d_3
dense_1	(None,128)	67108992	flatten_1
s_mean	(None,16)	2064	dense_1
s_log_var	(None,16)	2064	dense_1
s (Lambda)	(None,16)	0	s_mean, s_log_var
Decoder			
z_sampling	(None,32)	0	z, s (concatenated)
dense_2	(None,128)	4224	z_sampling
dense_3	(None,524288)	67633152	dense_2
reshape	(None,16,16,16,128)	0	dense_3
conv3d_transpose	(None,32,32,32,32)	110624	reshape
conv3d_transpose_1	(None,64,64,64,16)	13840	conv3d_transpose
decoder_output	(None,64,64,64,1)	433	conv3d_transpose_1

Supplementary Table 6.
Architecture of the VAE model

Layer	Output Shape	# Param	Connected to
Encoder			
encoder_input	(None,64,64,64,1)	0	-
conv3d	(None,32,32,32,96)	2,688	encoder_input
conv3d_1	(None,16,16,16,192)	497,856	conv3d
flatten	(None,786432)	0	conv3d_1
dense	(None,128)	100,663,424	flatten
z_mean	(None,32)	4128	dense

z_log_var	(None,32)	4128	dense
z (Lambda)	(None,32)	0	z_mean, z_log_var
Decoder			
z_sampling	(None,32)	0	z
dense_1	(None,128)	4224	z_sampling
dense_2	(None,786432)	101,449,728	dense_1
reshape	(None,16,16,16,192)	0	dense_2
conv3d_transpose	(None,32,32,32,192)	995,520	reshape
conv3d_transpose_1	(None,64,64,64,96)	497,760	conv3d_transpose
decoder_output	(None,64,64,64,1)	2,593	conv3d_transpose_1

Supplementary Table 7.
Anatomical Labeling of AAL90 Regions

Index	Region Name	Abbreviation
1,2	Precentral Gyrus	PreCG.L/R
3,4	Superior Frontal Gyrus, Dorsolateral	SFGdor.L/R
5,6	Superior Frontal Gyrus, Orbital Part	ORBsup.L/R
7,8	Middle Frontal Gyrus	MFG.L/R
9,10	Middle Frontal Gyrus, Orbital Part	ORBmid.L/R
11,12	Inferior Frontal Gyrus, Opercular Part	IFGoperc.L/R
13,14	Inferior Frontal Gyrus, Triangular Part	IFGtriang.L/R
15,16	Inferior Frontal Gyrus, Orbital Part	ORBinf.L/R
17,18	Rolandic Operculum	ROL.L/R
19,20	Supplementary Motor Area	SMA.L/R
21,22	Olfactory Cortex	OLF.L/R
23,24	Superior Frontal Gyrus, Medial	SFGmed.L/R
25,26	Superior Frontal Gyrus, Medial Orbital	ORBsupmed.L/R
27,28	Gyrus Rectus	REC.L/R
29,30	Insula	INS.L/R
31,32	Anterior Cingulate and Paracingulate Gyri	ACG.L/R
33,34	Median Cingulate and Paracingulate Gyri	DCG.L/R
35,36	Posterior Cingulate Gyrus	PCG.L/R
37,38	Hippocampus	HIP.L/R
39,40	Parahippocampal Gyrus	PHG.L/R
41,42	Amygdala	AMYG.L/R
43,44	Calcarine Fissure and Surrounding Cortex	CAL.L/R

45,46	Cuneus	CUN.L/R
47,48	Lingual Gyrus	LING.L/R
49,50	Superior Occipital Gyrus	SOG.L/R
51,52	Middle Occipital Gyrus	MOG.L/R
53,54	Inferior Occipital Gyrus	IOG.L/R
55,56	Fusiform Gyrus	FFG.L/R
57,58	Postcentral Gyrus	PoCG.L/R
59,60	Superior Parietal Gyrus	SPG.L/R
61,62	Inferior Parietal Lobule (Supramarginal)	IPL.L/R
63,64	Supramarginal Gyrus	SMG.L/R
65,66	Angular Gyrus	ANG.L/R
67,68	Precuneus	PCUN.L/R
69,70	Paracentral Lobule	PCL.L/R
71,72	Caudate Nucleus	CAU.L/R
73,74	Putamen	PUT.L/R
75,76	Pallidum	PAL.L/R
77,78	Thalamus	THA.L/R
79,80	Heschl's Gyrus	HES.L/R
81,82	Superior Temporal Gyrus	STG.L/R
83,84	Temporal Pole: Superior Temporal Gyrus	TPOsup.L/R
85,86	Middle Temporal Gyrus	MTG.L/R
87,88	Temporal Pole: Middle Temporal Gyrus	TPOmid.L/R
89,90	Inferior Temporal Gyrus	ITG.L/R

Supplementary Table 8.

Anatomical Mapping of SUIT Regions

Index	Region Name	Abbreviation	Anatomical Position
1-2	Cerebellum I-IV (Left/Right)	I-IV.L/R	Anterior Lobe of Cerebellum
5-6	Cerebellum V (Left/Right)	V.L/R	Central Portion of Anterior Lobe
7-8	Cerebellum VI (Left/Right)	VI.L/R	Posterior Lobe of Cerebellum
9-10	Crus I (Left/Right)	CrusI.L/R	Lateral Zone of Cerebellum
11-12	Crus II (Left/Right)	CrusII.L/R	Posterior Part of Lateral Zone
13-14	Lobule VIIb (Left/Right)	VIIb.L/R	Inferior Portion of Posterior Lobe
15-16	Lobule VIIIa (Left/Right)	VIIIa.L/R	Medial Portion of Posterior Lobe
17-34	Deep nuclei (e.g. dentate nucleus)	DN/Fast.L/R	Deep Cerebellar White Matter

Supplementary Figures

Supplementary Figure 1. Site-specific Representational Similarity Profiles of Shared and MCI-specific Features.

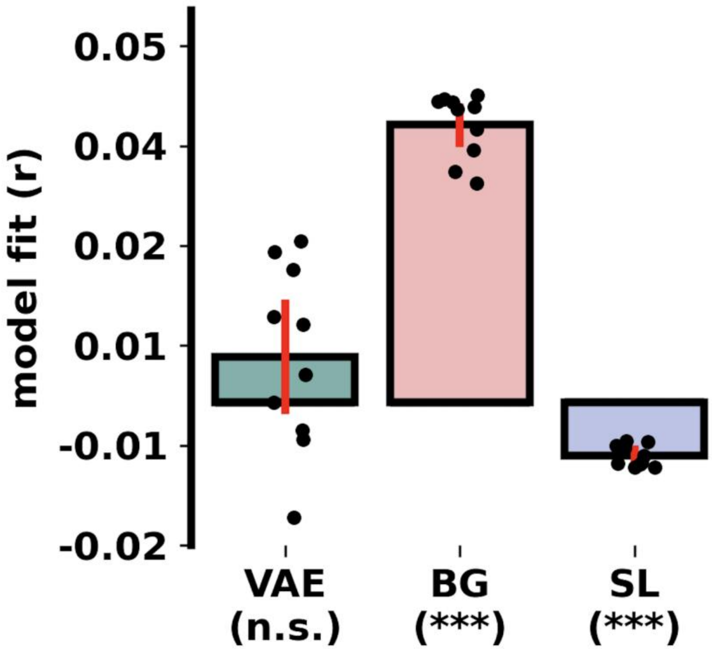

Supplementary Figure 2. The Impact of KL Divergence Weight Coefficient (β) on the Stability of Cognitive Domain Feature Disentanglement. The figure presents an analysis of how the KL divergence weight coefficient (β) in the Conditional Variational Autoencoder influences the stability of feature disentanglement across different cognitive domains. The Δτ values on the Y-axis represent the correlation differences between MCI-specific latent features and shared latent features in capturing each cognitive domain.

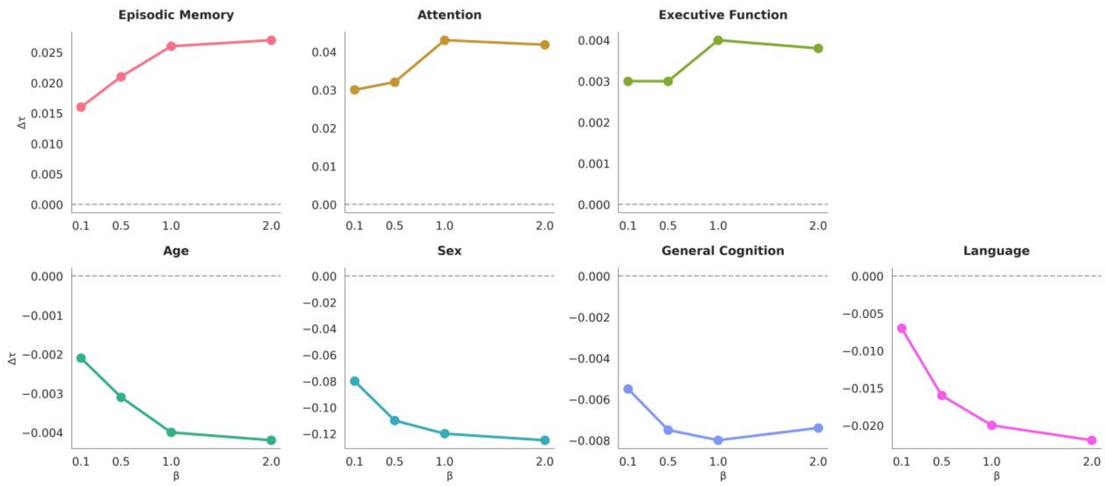

Supplementary Figure 3. Impact of Latent Space Dimension on the Stability of Cognitive Domain Feature Disentanglement. This figure shows how the latent space dimensionality of the Conditional Variational Autoencoder affects the stability of feature disentanglement across various cognitive domains. The Δτ values on the Y-axis represent the differences in correlation between MCI-specific and shared latent features in capturing each cognitive domain. Results indicate stable performance throughout the tested dimensional range (16 – 48), suggesting that the model' s ability to isolate MCI-specific neuroanatomical features is generally robust to the choice of latent dimension.

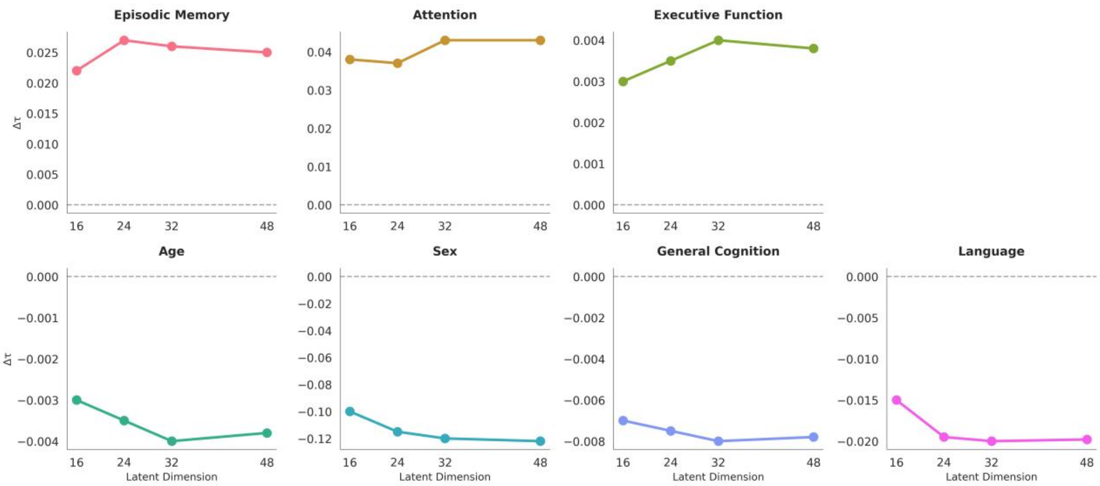

Supplementary Figure 4.Conceptual illustration of disease-free brain reconstruction and MCI-specific structural deformation extraction. This figure illustrates the core analytical pipeline for quantifying MCI-specific brain alterations. For each MCI subject, the encoder disentangles the input brain morphology into a shared latent representation, which captures non-disease-related variation, and an MCI-specific latent representation. Decoding the shared representation alone generates a subject-specific, counterfactual "disease-free" baseline by effectively removing the modeled MCI-specific components. Decoding the combined latent representation reconstructs the subject' s observed disease state. The deformation field (Φ) computed between these two reconstructions quantifies the subject-specific structural deviation attributable to MCI. Aggregating these deformation fields across the cohort using leave-one-subject-out principal component analysis (LOSO-PCA) yields robust, group-level MCI-specific structural maps, as reported in the Results. Thus, the "disease-free" brain is operationalized as a personalized statistical counterfactual rather than a real healthy control. Its systematic comparison with the observed disease state enables the isolation of disease-specific features and the identification of consistent group-level MCI-specific patterns highlighted in this study.

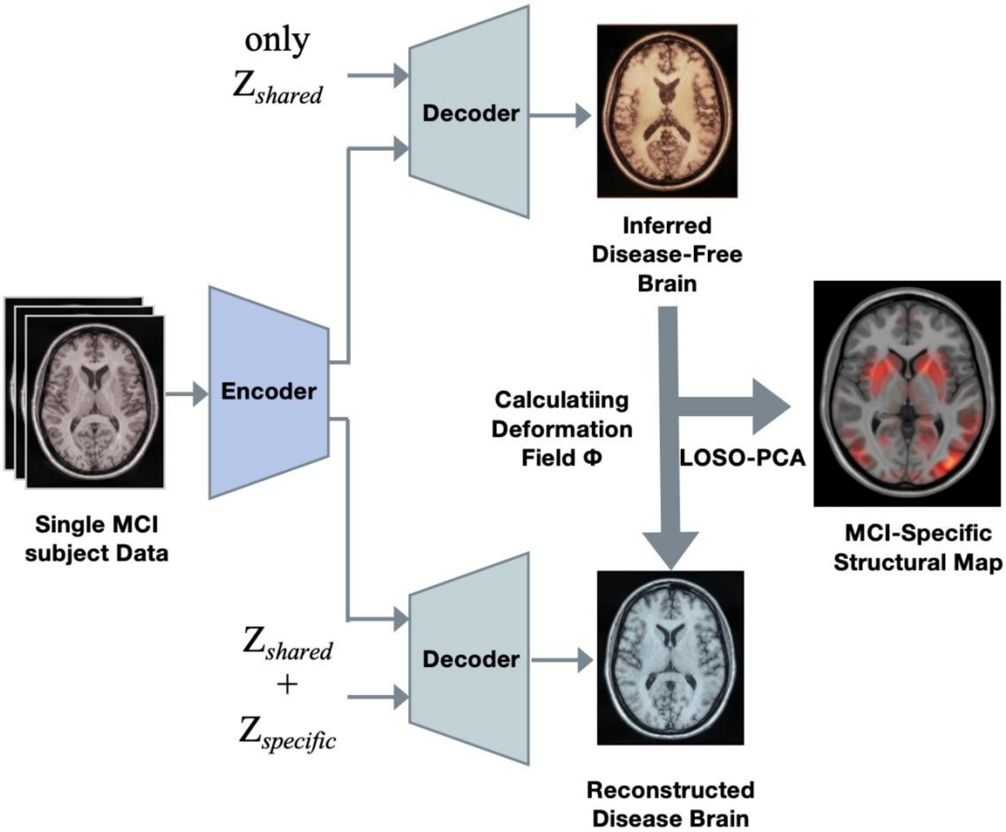

Supplementary Figure 5. Optimal Threshold Determination of Specific Features Based on Performance Metrics.